Insights into the response of *Miscanthus x giganteus* to rhizobacteria: enhancement of metal tolerance and root development under heavy metal stress

Mila Pešić[1,2], Svetlana Radović[1,4], Tamara Rakić[1], Željko Dželetović[3], Slaviša Stanković[1,4] and Jelena Lozo[1,4,*]

[1]*University of Belgrade – Faculty of Biology*, Belgrade, Serbia

[2]*Institute of Soil Science, University of Belgrade*, Belgrade, Serbia

[3]*Institute for the Application of Nuclear Energy, University of Belgrade*, Belgrade, Serbia

[4]*University of Belgrade – Faculty of Biology, Centre for Biological Control and Plant Growth Promotion*, Belgrade, Serbia

*Corresponding author: jlozo@bio.bg.ac.rs

Abstract: The use of bioenergy crops such as *Miscanthus x giganteus* in phytoremediation could have both environmental and economic benefits, such as biomass production and soil conservation for crops. In our previous work, we showed that rhizobacteria from the rhizosphere of *M. x giganteus* stimulated metal extraction and uptake and enhanced the phytoremediation ability of treated *M. x giganteus*. In the present study, we conducted transcriptome analysis and qPCR to elucidate the molecular mechanisms underlying these interactions in response to bacterial treatment by identifying the candidate genes involved in growth and development processes and metal uptake. Using high-throughput RNA sequencing of root samples, we found that 5134 and 4758 genes were up- and downregulated in plants treated with the rhizobacteria consortium. Gene ontology analysis showed that the upregulated DEGs were significantly enriched in 32 terms, while the downregulated genes were significantly enriched in 63 terms. Our results confirmed the increased expression of two genes: the multidrug and toxic compound extrusion, also known as multi-antimicrobial extrusion *(MATE) 40*, known for its role in plant response to biotic and abiotic stress, and *COBRA-like protein 1* belonging to the COBRA-like (COBL) gene family, which encodes a putative glycosylphosphatidylinositol (GPI)-anchored protein involved in cell wall thickening, cell elongation, and biomass increase when compared to untreated plants. We present the first insight into a mechanism whereby the interaction between the rhizobacterial consortium and *M. x giganteus* fosters plant growth and enhances its capacity for phytoremediation.

Keywords: microorganisms-plant interactions; transcriptome analysis; differential gene expression (DEG); phytoremediation; *Miscanthus x giganteus*

INTRODUCTION

Plant growth-promoting (PGP) bacteria are a heterogeneous group of beneficial microorganisms present in the root zone (rhizosphere), leaves (phyllosphere), or plant internal tissue (endosphere). Some of the known PGP properties of these bacteria may act as biostimulants through direct or indirect mechanisms of growth promotion, such as the production of phytohormones, such as indole-3-acetic acid, cytokinins, gibberellins, and secretion of 1-aminocyclopropane-1-carboxylate deaminase. They can also serve as biofertilizers, enhancing nutrient availability, or indirectly as biocontrol agents by generating antibiotics, hydrolytic enzymes, hydrocyanic acid, or inducing systemic resistance [1,2]. The rhizosphere is a soil region of great importance for plant-microorganism interactions, root function, and plant nutrition and health. The composition and structure of microbial communities in the rhizosphere are strongly influenced by root exudate composition but also by plant species, soil type, nutritional status, and other environmental factors [3,4]. Root exudate composition is also affected by environmental stimuli, but how this influences the microorganisms in the rhizosphere needs further study. The plant microbiome, together with PGP rhizobacteria, contributes to the resistance of plants to biotic and abiotic stressors and helps them survive under adverse conditions,

such as those with elevated concentrations of heavy metals. Different rhizobacterial strains stimulated the growth of essential vegetable crops such as *Lycopersicon esculentum* [5], *Triticum aestivum* [6], *Oryza sativa* [7], *Solanum nigrum* [8], *Helianthus annuus* [9], *Raphanus raphanistrum* subsp. *sativus* [10], etc., growing in soils contaminated with heavy metals. However, these inoculants had different effects on the bioavailability of metals, as some promoted the uptake and accumulation of heavy metals in plant tissues, and others decreased it. Therefore, bacterial strains that reduce the uptake of heavy metals by plants are preferable for agriculture purposes, particularly when lower concentrations of heavy metals are sought, especially in the edible parts of a plant. Conversely, bacterial strains that stimulate phytoextraction and phytostabilization are better suited for application in phytoremediation. Mechanisms used by metal-resistant PGP rhizobacteria to mobilize metals and increase their bioavailability generally involve rhizosphere acidification, the secretion of various organic acids and biosurfactants to enhance solubilization and the expansion of root surface area for increased metal absorption. Although these bacteria employ mechanisms resulting in reduced metal bioavailability, such as biosorption and bioaccumulation, precipitation, complexation, and alkalinization processes, they also facilitate metal sequestration through the secretion of extracellular polymeric substances (EPS) and facilitate metal transformation via oxidation-reduction reactions. [11,12]. However, the exact molecular mechanisms behind these interactions between microorganisms and plants have not been sufficiently investigated and understood, leaving many aspects still unknown.

Miscanthus x giganteus, a triploid hybrid, is tolerant to various abiotic stresses, including high metal concentrations [13,14], a wide range of temperatures [15], and organic pollution [16]. Due to its remarkable hardiness and high photosynthetic capacity at low temperatures, *M. x giganteus* is a desirable biofuel crop for marginal lands in a temperate climate grown for phytoremediation and biomass production. Plants suitable for phytoremediation should be fast-growing, provide high biomass yield and be easy to harvest, have well-developed root systems, be tolerant to heavy metals, and be capable of accumulating them in large quantities [17]. However, Fernando and Oliveira [18] found that the productivity and biomass quality of *M. x giganteus* were significantly affected by the heavy metal type and its interaction with other

nutrients such as Ca, K, and Mg. Phytoremediation, as a form of bioremediation, is an environmentally friendly approach based on the use of plants and their associated rhizospheric microorganisms for *in situ* stabilization, transformation, or degradation of pollutants in the environment. The importance of PGP rhizobacteria for phytoremediation has been documented in previous studies [19], but studies on the effect of PGP on *M. x giganteus*, especially in contaminated soils, are scarce. Most of the papers published to date have focused on the effects of *M. x giganteus* on microbial community establishment [16,20] or of heavy metals on *M. x giganteus* microbiome establishment [21]. The ability of *M. x giganteus* to augment phytoremediation is influenced by its associated microbiome, especially under heavy metal stress. Zadel et al. [21] found that certain rhizobacteria, such as *Luteolibacter* and *Micromonospora*, were enriched and highly abundant under heavy metal stress, which could improve plant performance. In the study by Pidlisnyuk et al. [22], inoculation of rhizomes with the *Bacillus altitudinis* K-14 strain increased the biomass of stems, leaves, and roots of *M. x giganteus* and influenced phytoremediation properties by improving the plant's potential for phytostabilization. Our previous study [23] showed that inoculation of *M. x giganteus* with PGP drought-adapted, heavy metal tolerant rhizobacteria isolated from its rhizosphere while growing in flotation tailings promoted lateral root development and root hair length and that root and shoot biomass and metal and P extraction rates were higher compared to non-inoculated control plants. As a result, inoculated *M. x giganteus* plants extracted higher total amounts of metals than control plants. Based on these observations, the objective of the current study was to explore the molecular basis of these processes, and the involvement of bacterial inoculation in the growth, development, and enhanced phytoremediation of *M. x giganteus*. Another unique feature of this study, as well as the previous one, is that they were carried out on a substrate obtained from flotation tailings of a mine rather than on soil contaminated with heavy metals. Therefore, we focused on two questions: (i) whether the interaction with rhizobacteria produces differential gene expression between control and treated *M. x giganteus* plants; (ii) in the genes that are responsive to this interaction, whether some could affect plant growth and development alongside higher heavy metal accumulation.

MATERIALS AND METHODS

Pot experiment design

The bacterial strains used to prepare the bacterial inoculum for this experiment were isolated, identified, and characterized in our previous work [23] and prepared as described. Briefly, selected rhizobacteria (*Pseudomonas chlororaphis* Bo, *Bacillus toyonensis* Co, *B. safensis* Do, *Arthrobacter* sp. B21, *B. aryabhattai* B22, and *B. thuringiensis* F4) were cultivated in LB media for 16 h at 30°C with shaking at 180 rpm. Cultures were then diluted to achieve a final OD600 of 1. The bacterial inoculum was prepared by mixing equal volumes of each bacterial culture. The substrate of flotation tailing was taken from a lead-zinc-copper mine in central Serbia (44°06'N, 20°29'E), homogenized by intensive mixing, and air-dried for two weeks. Three kg of the substrate was added to each pot. The rhizomes of *M. x giganteus* used in this experiment were obtained from the experimental plot of INEP Belgrade, Serbia (44°51'N, 20°22'E), where *M x giganteus* has been continuously grown in uncontaminated soil since 2007. After removal from the soil, rhizomes were thoroughly washed with tap water, cut to a similar weight, and then left in the dark for 7 days. Rhizomes of similar weight (20-25 g) and several buds were surface sterilized in 0.8% sodium hypochlorite for 15 min and washed several times with sterile water. The surface-sterilized rhizomes were immersed in the prepared bacterial inoculum (plants labeled mix) or in sterile lysogeny broth (LB) medium (plants labeled control) and incubated for 1 h. After incubation, 1 rhizome per pot was planted in pots with the substrate, and 50 mL of the bacterial inoculum or LB medium was added to the substrate surrounding the rhizome. Plants were cultivated for 3 months in a growth box under controlled conditions: a 16/8 h photoperiod, 22°C, humidity 35%, and regular irrigation (150 mL tap water in 72 h). Pots were randomly placed in the growth box. Five rhizomes were planted for each experimental group. After 3 months of growth, the plants were harvested. Some of the roots and leaves were immediately washed firstly with tap water and then sterilized distilled water and ground in liquid nitrogen using a mortar and pestle. The rest of the roots and leaves, as well as the stems and rhizomes, were air-dried until they attained a constant weight and then used to determine the concentrations of microelements.

Plant growth parameters

Shoots were separated from roots, and the roots were washed thoroughly in tap water and then rinsed in deionized water. Root parameters, including total length, main and lateral root lengths, fresh mass, and dry mass, were measured. Shoot characteristics such as the number of leaves per shoot, shoot length, and fresh and dry mass of leaves and stems were also recorded. Plant growth inhibition (%) was calculated using the following formula:

$$\text{plant growth inhibition (\%)} = [((\text{dry mass (treatment)} \times 100)/ (\text{dry mass (control)}))-100].$$

Determination of different elements in plant organs

The powder obtained from ground plant organs was entirely digested with 65% HNO_3 according to method 3051 (USEPA 1998). The concentrations of microelements (Cu, Zn, Mn, Ni) and toxic non-essential elements (Pb, Cd, Cr) were determined using an atomic absorption spectrophotometer (Shimadzu AA 7000) and known standards for comparison of absorbance values. The results of the analysis of soil and plant element content were used to calculate the bioconcentration factor (BCF), translocation factor (TF), and uptake index using the following equations [22]:

$$BCF=(\text{element content in plant tissues (mg/kg)})/ (\text{original element content in soil (mg/kg)})$$

$$TF=(\text{element content in aboveground biomass of plants (mg)})/(\text{element content in roots (mg)})$$

$$\text{Uptake index (mg)}=\text{concentration of element (mg/kg)} \times \text{Dry weight (kg)}.$$

RNA extraction and sequencing

The roots of the two experimental treatments (mix and control) were cut when the plants were still intact, washed thoroughly with tap water and sterilized distilled water, and immediately crushed in liquid nitrogen with a mortar and pestle. 70-80 mg of the plant material was collected for total RNA extraction using the RNeasy® Plant Mini Kit (QIAGEN, Hilden, Germany) according to the manufacturer's instructions. The purity, integrity, and concentration of isolated RNA

were determined using a NanoPhotometer spectrophotometer (IMPLEN, Munich, Germany). Samples were stored at -80°C. Sequencing of mRNA from the collected samples was performed on the NovaSeq 6000 PE150 platform (Novogene Co. Ltd. Cambridge, U.K.)

Data and enrichment analysis

The raw data were processed through filters to remove reads of insufficient quality. The clean reads obtained were used to calculate Q20, Q30, and GC content [24-26]. A reference genome of *M. x giganteus* was not available, so alignment with the genome of *M. x lutarioriparius* was performed using HISAT2 software. String tie was used to assemble the set of transcript isoforms of each bam file obtained in the mapping step. Feature counts were used to count the mapped read numbers of each gene, including both known and new genes. Then, the RPKM of each gene was calculated based on the length of the gene and the number of reads mapped to that gene [27]. Before differential gene expression (DEG) analysis, read counts for each sequenced library were adjusted by trimmed mean of M values (TMM) with a scaling normalization factor [28]. DEG analysis of untreated and treated plants was performed using the DGESeq R package, and P values were adjusted using the method of Benjamini and Hochberg [29]. A corrected P value of 0.005 and |log2 (fold change) of 1 were set as thresholds for the significant DEGs [30]. The enrichment analysis of DEGs in the Gene Ontology (GO) was performed using the cluster Profiler R package. GO Terms with a corrected P value of less than 0.05 were considered significantly enriched by DEGs. The cluster Profiler R package was used to test the statistical enrichment of genes with differential expression in KEGG pathways [31,32].

Quantitative PCR (qPCR) analysis of selected differentially expressed genes (DEGs)

Quantitative PCR (qPCR) was used to verify the upregulation of selected transcripts detected as DEGs by RNA sequencing. Four transcripts were selected based on GO enrichment analysis, and the P values were adjusted for multiple testing (padj) of MATE protein 14, MATE protein 40, COBRA-like protein 1, and chitinase-like protein 1. Primers for the selected transcripts are listed in Supplementary Table S1. The

RevertAid First Strand cDNA Synthesis Kit (Thermo Fisher Scientific; Waltham, MA, USA) was used to synthesize cDNA from total RNA isolated from *M. x giganteus* roots as described previously and according to the manufacturer's instructions. The qPCR reaction was performed using SYBR Green Master Mix (Applied Biosystems, Thermo Fisher Scientific) and run on a 96-well real-time PCR instrument, the StepOnePlus™ Real-Time PCR System (Applied Biosystems, Thermo Fisher Scientific). Both experimental groups (mix and control) had three biological replicates, and each was run in two technical replicates. Thermal conditions included initial denaturation at 95°C for 10 min, 40 cycles at 95°C for 15 s, and 60°C for 1 min. The expression ratio between mix and control samples for the selected transcripts, normalized to the *Sb02g041180* gene as a reference, was calculated using the Pfaffl method [33].

Identification of *MATE* and *COBRA-like* genes in the *Miscanthus lutarioriparius* genome

Since no *M. x giganteus* genomic data is available, we assumed that the closest available genome is the reference genome of *M. lutarioriparius*, which was used for *MATE* and *COBRA-like* gene search (GenBank GCA_904845875.1, available at https://www.ncbi.nlm.nih.gov) [34]. The consensus sequences of MatE and COBRA domains were obtained from the Conserved Domain Database (CDD, https://www.ncbi.nlm.nih.gov/Structure/cdd/) and used as queries for BLASTP search against the reference proteome of *M. lutarioriparius*. To obtain more accurate numbers of *MATE* and *COBRA-like* genes, BLASTP hits were manually filtered by the presence of conserved MatE (Pfam: PF01554) or COBRA (Pfam: PF04833), respectively, using the HMMER (https://www.ebi.ac.uk/Tools/hmmer/ search/hmmscan) and the Conserved Domain Database (CDD, https://www.ncbi.nlm.nih.gov/Structure/cdd/). Putative MATE sequences were also assessed for typical features of the plant MATE transporters, such as the presence of the MatE domain, 8-12 transmembrane domains, and classification as MATE_like superfamily [35]. Physical parameters such as molecular weight (MW), theoretical isoelectric point (pI), total number of negatively charged residues (Asp+Glu), total number of positively charged residues (Arg+Lys), instability index, aliphatic index, and grand average of hydropathicity (GRAVY) were determined by ProtParam (https://web.expasy.

org/protparam/). The subcellular localization was predicted using Plant-mPLoc (http://www.csbio.sjtu.edu.cn/bioinf/plant-multi/).

Phylogenetic analysis

Fifty-six MATE and 12 COBRA-like sequences from *Arabidopsis thaliana* were downloaded (https://www.ncbi.nlm.nih.gov, TAIR: http://www.arabidopsis.org) and used for the construction of two phylogenetic trees together with the MATE and COBRA-like sequences obtained from *M. lutarioriparius* after filtering the BLASTP data. MEGA X software (www.megasoftware.net) was used for the phylogenetic tree construction following the maximum likelihood method. Parameters applied were as follows: Test of phylogeny: Bootstrap method, Number of bootstrap replications: 1000, Substitutions type: Amino acid, Model/method: Jones-Taylor-Thornton (JTT) model, Rates among sites: Uniform rates, Gaps/missing data treatment: Complete deletion, ML heuristic method [36].

Statistical analysis

All tests were performed with at least three biological replicates and repeated in at least two technical replicates. The data obtained were first tested for equality of variance using Levene's test and for normality using the Shapiro-Wilk test. The data were then subjected to a one-way analysis of variance (ANOVA), and the means were compared using Student's t-test, with significance at $P<0.05$. All statistical analyses and data visualization were performed in Python version 3.9.7, available at https://www.phyton.org, using appropriate libraries [37,38].

RESULTS

Impact of bacterial consortium treatment on growth parameters and metal uptake in *M. x giganteus*

Compared to the control, the plants treated with a consortium of bacteria looked much healthier, with more leaves per stem and fewer senescent leaves (data not shown), which was also linked to earlier germination (one month earlier) and a higher germination rate (100% of planted rhizomes in the mix compared to 60% in the control). The treated plants (mix) also
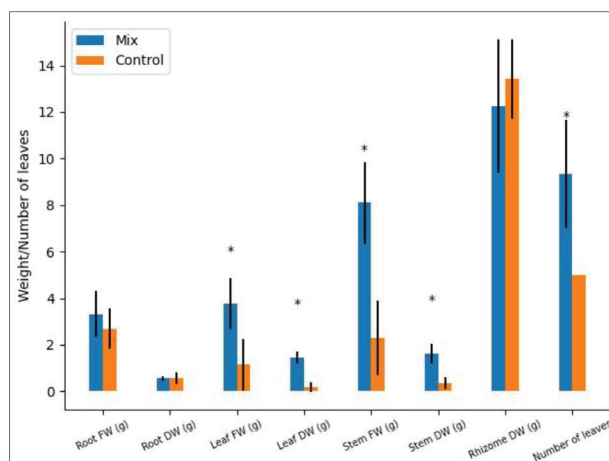

Fig. 1. Growth parameters 1. Weight and number of leaves. Data are presented as the mean±SD. Asterisks indicate statistically significant differences between the control and mix (Student's t-test, *$P<0.05$). DW – dry weight, FW – fresh weights.
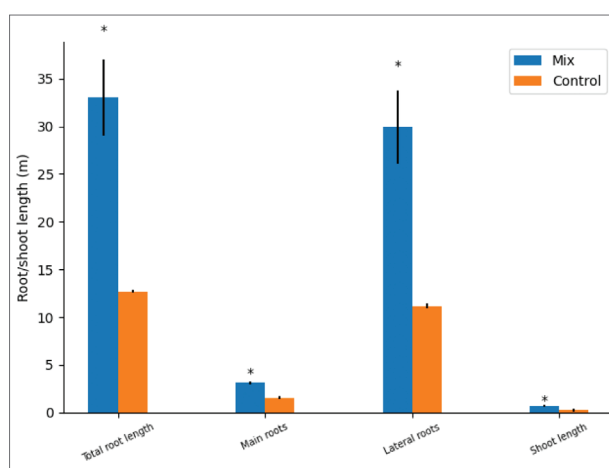

Fig. 2. Growth parameters 2. Root and shoot length. Data are presented as the mean±SD. Asterisks indicate statistically significant differences between the control and mix (Student's t-test, *$P<0.05$).

had significantly longer stems and more leaves per stem, increasing the aboveground biomass, which was reflected in significantly higher fresh and dry weights of leaves and stems (Fig. 1). As can be seen from the photos of the washed roots, the root system of the treated plants was significantly enhanced compared to the control (Supplementary Fig. S1). The total length of the roots measured in the mixture was significantly greater than that of the control plants. In addition, the plants treated with bacteria had significantly longer main and lateral roots compared to the untreated plants (Fig. 2). Total biomass production was 233% higher in the bacteria-treated plants than in the control plants.
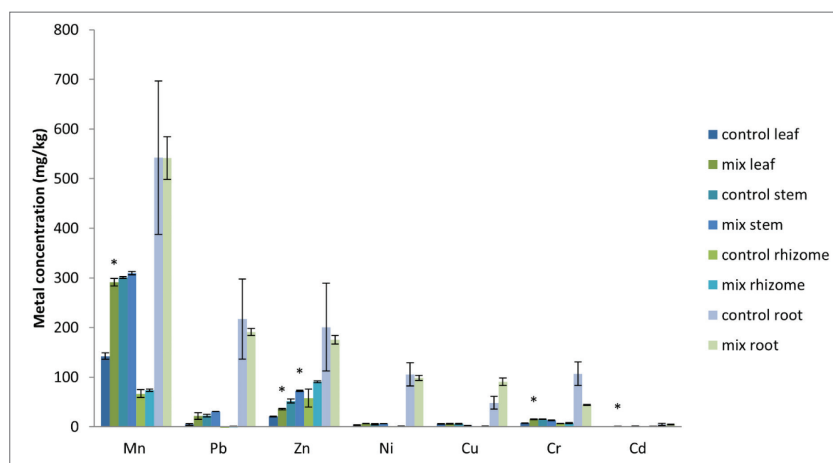
Fig. 3. Metal concentrations in plant organs of *M. × giganteus* in two experimental groups (control and mix). Data are presented as the mean±SD. Asterisks indicate statistically significant differences between the two groups, control and mix (Student's t-test, *P<0.05).

Metal concentrations in different plant parts are shown in Fig. 3. *M. x giganteus* plants, both treated with the bacterial consortium and untreated plants, exhibited several-fold higher metal accumulation in their roots compared to their aboveground organs, such as leaves or stems, with the most significant differences observed for Ni, Pb, Cu, and Cd. The concentrations of Pb in the rhizomes of both mix and control and of Ni in the rhizomes of the control were below the detection limit. Of all metals tested, the *M. x giganteus* plants accumulated considerably more Mn than other metals in both experimental groups, with the greatest difference found in leaves and stems. The only exception was the rhizome of the mix, which had a higher amount of Pb than Mn. Compared to the control plants, the plants treated with the bacterial consortium had significantly higher concentrations of Mn, Zn, Cr, and Cd in the leaves and Zn in the stems.

The concentration of accumulated metal in each plant organ was in the following order: root>stem>leaf>rhizome for Mn, Pb, Ni, and Cd in both samples and of Cu and Cr only in the control; for the mix, the order for Cu was root>leaf=rhizome>stem, while for Cr the order was root>leaf>stem>rhizome; for Zn, the order was root>rhizome>stem>leaf for both samples. However, the total amount of extracted metals expressed as the uptake index (Table S2) was highest in the rhizome for Mn, Zn, Cu, and Cr in both the control and the mix and for Cd only in the mix. The highest uptake index was found in the roots of

both samples for Pb and Ni and for Cd in the control sample. Treatment with the selected rhizobacterial consortium stimulated the translocation of all analyzed metals to the aerial parts, leaves, and stems, as evidenced by a higher uptake index compared to the control (Table S2). The capacity of plants for phytostabilization or phytoextraction is estimated by translocation factors (TLF) (Supplementary Table S3), calculated as the ratio between the content of metals in the aboveground biomass of the plant (stems and leaves) and in the roots. Bacterial treatment increased TLF values for all metals tested, and these values were higher than 1 for Mn, Zn, Cr, and Cd, increasing the phytoextraction potential of *M. x giganteus*.

Transcriptome sequencing and determination of DEGs

For this study, the total RNA samples were obtained from the roots of plants treated with bacterial consortium (mix) and not treated (control). cDNA libraries were prepared and then sequenced using the Illumina sequencing platform. Sequencing results are summarized in Supplementary Table S4. After RNA-seq, the number of raw data was 21,146,651 and 22,713,862 for the control and the mix, respectively. Data obtained for clean reads, GC content, and Q20 and Q30 parameters were similar for both libraries, and the data quality was good enough for further analysis. The total mapping rate of clean reads against the *M. lutarioriparius* genome showed that at least 87.36% and 87.07% were mapped for the control and the mix, respectively; 78.53% and 77.20% of the total reads for the control and the mix were uniquely mapped reads, respectively. Fragments per kilobase of transcript per million mapped reads (FPKM) were calculated based on gene length and sequencing depth and used as a measure of gene expression. The Venn diagram (Fig. 4A) shows co-expressed and uniquely expressed genes in the roots of both experimental groups, while 31,996 and 37,087 genes were found in the control and the mix, respectively. The DEGs were analyzed by comparing control and mix, using a padj value of 0.005 and a
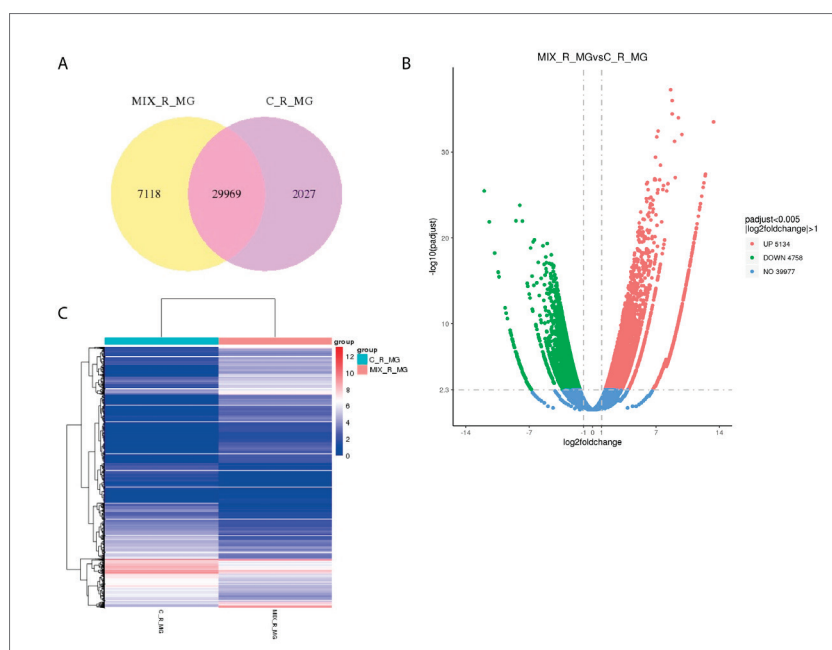
Fig. 4. A – Venn diagram showing co-expressed and uniquely expressed genes in two experimental groups (control and mix). **B** – Volcano plot showing the number of differentially expressed genes (DEGs) between two experimental groups. DEGs between the two experimental groups were calculated using the package edgeR with threshold padj≤0.005 and log2FoldChange≥1.0. **C** – Hierarchical clustering of DEGs between the mix and the control. Blue and red colors indicate low and high expressions, respectively.
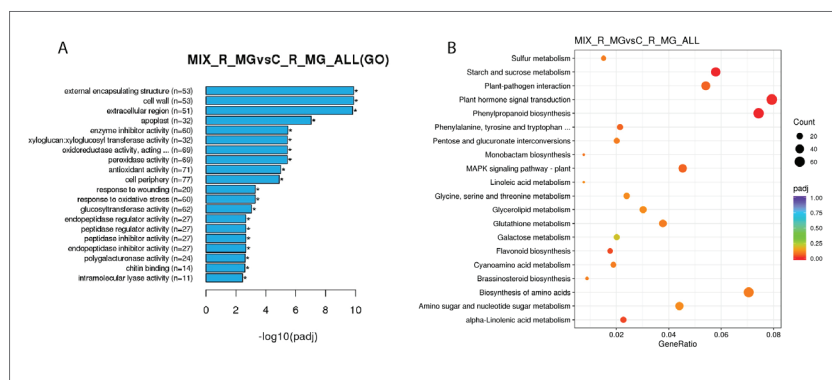

Fig. 5. A – Summary Gene Ontology (GO) enrichment analysis of differentially expressed genes (DEGs). The length of the bars indicates the statistical significance of each GO term (*P<0.05). **B** – Summary KEGG enrichment analysis of DEGs. The gene ratio on the x-axis indicates the ratio of DEGs in the pathway to the total number of annotated genes in the pathway. The size of the dots represents the number of DEGs in the pathway, and the color of the dots represents the adjusted P value.

log2 fold change≥1 as parameters for significance. The volcano plot shows the number of DEGs in the mix compared with the control, revealing a slightly higher number of upregulated genes (Fig. 4B). The hierarchical clustering of DEGs showing their profiles in the roots of the control and mix is shown in Fig. 4C. The

list of 9,892 significant DEGs can be found in Supplementary Table S5. GO enrichment analysis was performed to annotate DEGs functionally. DEGs were classified into three groups: biological processes (BP), molecular function (MF), and cellular components (CC). The upregulated DEGs were significantly enriched in 32 GO terms, while the downregulated DEGs were significantly enriched in 63 GO terms. The summarized results for the 20 most enriched DEGs belonging to all three GO groups and the results of the KEGG (Kyoto Encyclopedia of Genes and Genomes) enrichment analysis showing the 20 most enriched metabolic pathways are given in Fig. 5A and B, respectively. One of the upregulated GO terms (GO:0042221) was classified as a reaction to chemicals. Among the DEGs significantly enriched in this GO were nine genes containing conserved domain features corresponding to proteins within the MATE protein family (PF01554). To validate the RNA sequencing results, qPCR analysis was performed for four selected genes: two belonging to the MATE family, *MATE 14* and *MATE 40*, that had the lowest padj values on RNA sequencing, and two encoding *COBRA-like protein 1* and *chitinase-like protein 1* that were also enriched in GO and reacted to the chemical. The qPCR analysis (Fig. 6) showed significantly higher expression of genes encoding MATE protein 40 and COBRA-like protein 1 in the mix compared with the control, which was consistent with the RNA-seq results. However, these results differed in the significance of fold change expression between mix and control: RNA-seq showed that *MATE 40* and *COBRA-like 1* genes had log2 fold change expression of 6.24 and 2.10, respectively, whereas
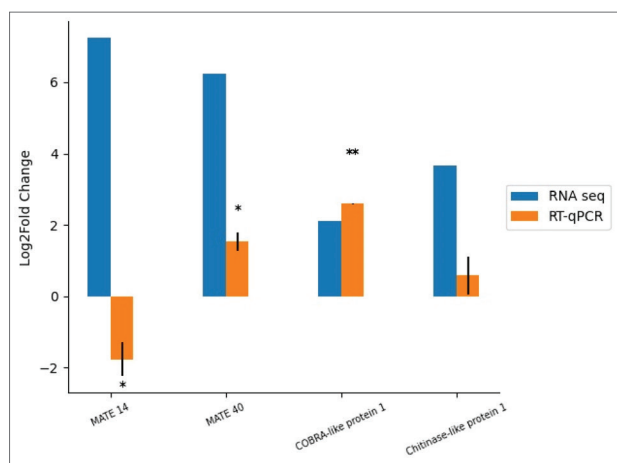
Fig. 6. Comparison of RNA sequencing and qPCR results for selected genes. Data for qPCR are shown as the mean±SEM. Asterisks indicate statistically significant differences between the two experimental groups, control and mix (Student's t-test, *P<0.05, **P<0.01).

qPCR showed that these values were 1.54 and 2.59. One gene, responsible for encoding MATE protein 14, exhibited significantly lower expression in the plants treated with bacterial inoculum compared to control plants when analyzed by qPCR, contrary to the results of RNA sequencing. The gene encoding chitinase-like protein 1 showed no statistically significant change in expression when analyzed by qPCR.

Identification of *MATE* and *COBRA-like* genes and phylogenetic analysis

Homology search and domain prediction (Pfam: PF01554) identified a total of 52 genes encoding MATE proteins, but after filtering by the presence of MatE and 8-12 transmembrane domains, the final number of genes in *M. lutarioriparius* was 49. The lengths of the predicted MATE proteins ranged from 400 to 603 aa, the molecular weights ranged from 43036.18 to 63540.86 D, and the predicted isoelectric points ranged from 5.34 to 9.79. Most of the proteins are neutral or partially alkaline (Supplementary Table S5). The predicted cellular locations of the MATE proteins were the cell membrane for 47 of the predicted proteins and the vacuole for 2 of the predicted proteins (Supplementary Table S5). The same was done for COBRA-like genes. Homology search and domain prediction (Pfam: PF04833) identified a total of 17 genes encoding COBRA-like proteins, but after

filtering by the presence of the COBRA domain, the final number of COBRA-like genes in *M. lutarioriparius* was 15. The lengths of the predicted COBRA-like proteins ranged from 360 to 678 aa, the molecular weights ranged from 40836.4 to 75101.24 D, and the predicted isoelectric points ranged from 5.35 to 9.05. Most of the proteins are partially alkaline or neutral (Supplementary Table S5). The predicted cellular location of all predicted proteins is in the cell membrane (Supplementary Table S5).

To investigate the phylogenetic relationship of the proteins of *M. lutarioriparius* MATE, a phylogenetic tree was constructed using the MATE sequences of *Arabidopsis thaliana* and the putative MATE sequences of *M. lutarioriparius*. According to the topology of the phylogenetic tree, the genes of *M. lutarioriparius* could be divided into four subgroups with 2, 10, 7, and 30 members. The transcripts upregulated in the mix compared to the control, as detected by RNA sequencing, matched the predicted proteins CAD6335071.1 and CAD6332924.1, which were grouped in the phylogenetic tree with the *A. thaliana* protein DETOXIFICATION 40 (AtDTX40) and the protein DETOXIFICATION 14 (AtDTX14), respectively (Supplementary Fig. S2). The predicted location of both proteins is the cell membrane (Supplementary Table S5). qPCR confirmed the upregulation of the gene encoding the protein DETOXIFICATION 40, but not the upregulated expression of the gene encoding the protein DETOXIFICATION 14.

In agreement with the orthologues in *A. thaliana*, the COBRA-like family members identified in *M. lutarioriparius* were clustered into two subgroups, with 13 genes belonging to subfamily 1 and 5 to subfamily 2 (https://www.arabidopsis.org/). One of the transcripts that showed upregulated expression in RNA-Seq analysis corresponded to the predicted protein CAD6223163.1, which was grouped with the COBL1 (COBRA-LIKE1) protein of *A. thaliana* (Accession: AAF02128) in the constructed phylogenetic tree (Supplementary Fig. S3). The predicted cellular location of this protein is the cell membrane (Supplementary Table S5). qPCR also confirmed the upregulation of this gene.

DISCUSSION

With industrial development and rapid population growth in recent decades, heavy metal pollution (HM) of soils has become a widespread problem. There are two approaches to remediation: *in situ* and *ex situ*, which can be carried out by physical, chemical, or biological methods [39]. Unlike physicochemical methods, bioremediation is a cost-effective and entirely environmentally friendly method that improves soil quality by increasing fertility and preventing erosion and metal leaching [40]. Plants and their associated microorganisms are key players in this process, and understanding the recruitment and factors through which plant growth-promoting rhizobacteria (PGPR) interact with plants is critical for bacteria-assisted phytoremediation. Our results document the positive effect on the growth parameters and accumulation of metals of *Miscanthus x giganteus* treated with a bacterial consortium from its rhizosphere. A study on the phytoremediation ability of *M. floridulus* shows that it largely depends on various ecological characteristics of the rhizosphere and other bacterial communities [41]. Bacterial inoculation of various species, such as *Salix atrocinerea*, improved plant growth parameters and the phytoremediation efficacy of trace elements [42]. Sometimes bacterial inoculation could lead to phytostabilization instead of phytoextraction by decreasing the translocation factor (TLF), and the uptake index of trace elements remains low, as documented in a study with *M. x giganteus* and *Bacillus altitudinis* K-14 strain [22]. However, unlike our study, which was conducted in the substrate obtained from the main flotation tailing, this study was conducted in contaminated soil. These completely different substrates for plant growth provide substantially different growth conditions, different initial communities of microorganisms, different nutrient availability, etc. Previous studies have demonstrated the significance of environmental factors such as soil properties, pollution levels, cultivation techniques, geographical location, and plant species as major contributors to the composition of the microbial community in the rhizosphere. [4,40]. The interaction between plants and microorganisms is bidirectional. The transcriptional response of *Pseudomonas putida* E36, isolated from *M. x giganteus* roots, was influenced by heavy metals, showing differences between exposure solely to heavy metals and exposure to both heavy metals and root exudates from heavy metal-treated *M. x giganteus*. [22].

Ezaki et al. [43] suggested that aluminum tolerance in *M. sinensis* and *Andropogon virginicus* involves at least three mechanisms: transport of toxic Al ions from roots to shoots, suppression of Al accumulation in root tips as these are the most important region for root growth, and suppression of oxidative damage through the expression of higher basal levels of superoxide dismutase and catalase after Al exposure. The activation of antioxidant enzymes and reduction of photosynthetic pigment concentration in *M. x giganteus* leaves when grown in metal-contaminated soil have also been reported [44]. To uncover the molecular mechanisms underlying metal uptake, transcriptome analysis of five *M. lutarioriparius* tissues was performed to investigate the correlation between the gene expression in rhizomes and its role in rhizome development and metal accumulation [45]. Transcriptome analysis of *M. sinensis* treated with 200 mg/l chromium (Cr) revealed 83,645 DEGs, many of which were responsible for heavy metal transport, chelation of metal ions, and photosynthesis [46]. Our study shows that treating *M. x giganteus* with its rhizobacterial consortium improved its growth and development, as shown in our previous study. Interestingly, the plants not only improved growth parameters but also better phytoremediation ability. Analysis of the transcriptome of *M. x giganteus* after treatment with rhizobacteria and without treatment revealed 9,892 DEGs. Using qPCR, we confirmed that the treated plants had induced the expression of two of the four genes analyzed. One of them, *MATE protein 40*, was involved in metal tolerance, and the other, *COBRA-like protein 1*, was involved in the root development of the plant. The MATE transporter family, originally described in bacteria as efflux transporters conferring drug resistance, is ubiquitously present in all prokaryotic and eukaryotic life forms. However, MATE underwent significant expansion in plants through tandem and segmental duplications not found in other organisms, indicating their importance to plant life [47]. MATE proteins are usually in plant membranes, performing important functions in plant growth and development. These include processes such as transporting secondary metabolites, toxic compounds, heavy metals, disease resistance, and regulating plant hormones [48,49]. The *MATE* genes constitute a family of multiple genes, with the number of genes varying among different plant species. Genome-wide and expression analyses have been performed on some economically important crops

such as potatoes [49], cotton [50], tomatoes [47], apples [35], rice [51], soybean [52], etc., as well as the model plant *A. thaliana* [52]. However, functional studies are still lacking, and the phylogenomic classifications available in the literature are not systematic. Genome-wide analysis of *MATE* genes has not been performed for any species in the *Miscanthus* genus. Hence, no information is available on the number, chromosome distribution, phylogenetic relationships, or expression patterns of genes. However, the importance of metal transporter genes for the phytoremediation potential of different *Miscanthus* species was also evident in the study by Guo et al. [54]. Transcriptome analysis of *M. sacchariflorus* and *M. floridulus* revealed distinct Cd-tolerant mechanisms, leading to significant differences in the expression of metal transporter genes. MATE proteins are associated with many processes, including organ differentiation, secondary metabolite transport, phytohormone transport, and ion homeostasis. As suggested by some of the studies conducted to date in various plant species, *MATE* genes are involved in plant responses to biotic and abiotic stresses [52]. However, the expression patterns of *MATE* genes depend on the plant species, specific stress conditions, tissue type, and developmental stage, as indicated by these studies. Huang et al. [49] investigated the relative expression levels of eight *stMATE* genes belonging to four different subfamilies in roots, stems, and leaves of *Solanum tuberosum* under heavy metal stress conditions after treatment with several metal species (Cu^{2+}, Cd^{2+}, Zn^{2+}, Ni^{2+}, and Pb^{2+}) for different periods. They found that the expression of the tested genes was upregulated in response to heavy metal stress, but the expression levels of each gene depended on the tissue type as well as the type of stressor and the duration of stress treatment. Sivaguru et al. [55] pointed out the important role of the plasma membrane-localized citrate efflux transporter encoded by the *SbMATE* gene in the apical region of roots of *Sorghum bicolor* in Al-induced stress tolerance. They found that Al stress-triggered expression of the *SbMATE* gene is localized in the cells of the root zone where the greatest Al-induced damage occurs, so that citrate excretion is localized in this specific zone, which is the mechanism that protects plant cells most sensitive to Al toxicity. They also found that root recovery coincides with *SbMATE* gene expression. Liu et al. [52] also pointed out the possible role of one of the *MATE* genes (*GmMATE75*)

expressed in soybean root tips in mediating soybean tolerance to Al toxicity. Zhang et al. [35] found that the expression of several *MdMATE* genes changed in apples in response to different pathogen species, indicating the role of these genes in managing biotic stress and disease resistance. They also found that the expression of *MATE* genes is dynamic in different tissues or developmental stages.

COBRA and *COBRA-like* (*COBL*) genes encode plant-specific glycosylphosphatidylinositol (GPI)-anchored proteins located at the interface of the plasma membrane and cell wall that have roles in cell expansion orientation and cellulose crystallinity status. *COBRA* genes belong to a multigene superfamily called the COBRA-like family, which has varying numbers of genes in different plant species [56]. The number of genes in this family varies among plant species and has additional specific plant species-dependent functions [57]. Ectopic expression of the cotton *COBL* gene *GhCOBL9A* in *A. thaliana* resulted in cell elongation, cell wall thickening, and biomass increase. Overexpression of this gene was also associated with the upregulation of cellulose synthase (*CesA*) genes and increased cellulose deposition [36]. The role of COBRA-like genes under stress conditions has also been reported. Zaheer et al. [58] identified five *COBL* genes in *Triticum aestivum,* and all of them responded to drought, which may indicate their role in stress tolerance. Bahmani et al. [59] showed that increased density and length of root hairs and increased ROS levels occurred in response to Cd. They showed that Cd and ROS downregulated the expression of three proline-rich elongation-like receptor kinases (PERK5, PERK8, and RHS10) but upregulated the expression of two elongation genes (*EXPA7* and *EXPA18*) and a *COBRA -like 9* (*COBL9*). In this study, we showed that expression of the *COBRA-like* gene was also increased in plants treated with rhizobacteria, leading us to conclude that these bacteria use mechanisms that ultimately lead to the activation of the *COBRA-like* gene. One of the consequences of this upregulation of members of the *MATE* and *COBRA-like* gene family could be significantly increased development of the root system in treated plants and increased tolerance to heavy metal-induced toxicity. Considering the importance of the root system in nutrient uptake and thus in plant growth and development, we believe that this indirectly influenced the higher biomass of the

treated plants. In this study, we focused on the root system because the results of our previous study showed increased formation of root hairs in bacteria-treated plants. We found two possible gene families involved in the observed phenomenon: *MATE* and *COBRA-like*. Nevertheless, the precise mechanisms and signaling events underlying this interaction, along with the involvement of other genes, remain to be elucidated in subsequent studies. Additionally, expression analysis of the entire family of *MATE* and *COBRA-like* genes in different organs of *M. x giganteus* and under diverse stress conditions could provide better insight into the function and regulation of these genes.

CONCLUSIONS

This study demonstrates the significant potential of treating *M. x giganteus* with a rhizobacterial consortium to enhance biomass production and metal extraction when grown in a substrate heavily contaminated with metals from mine flotation tailings. Transcriptome analysis showed that more than 9892 genes were differentially expressed between treated and control plants. Of the four genes selected for qPCR analysis, the results suggest the importance of the *MATE* and *COBRA-like* gene family in the mechanisms of tolerance to heavy metals and uptake by *M. x giganteus* in metal-contaminated soils. Based on our results, we propose that the interaction between rhizobacterial inoculants and *M. x giganteus* leads to the activation of *COBRA-like 1* and *MATE40* genes in *M. x giganteus* roots. We hypothesize that activating these genes will increase root resistance to metal toxicity, allowing for less root damage, better root growth, root hair development, and drought tolerance. Developed roots allow for a more efficient uptake of nutrients, ultimately leading to increased growth and biomass accumulation throughout the plant. Based on data available in the literature, we hypothesized that MATE transporter 40 plays a role in metal tolerance as well as metal transport across the cell membrane, whereas COBRA-like protein 1 is involved in root system developmental processes. As a result, treatment with a rhizobacterial consortium stimulated the increased growth of *M. x giganteus* and enhanced its phytoremediation ability. However, further transgenic studies are needed to confirm the function of these proteins. We highlight these results because the experiments were conducted in a substrate derived from mine flotation tailing, a sandy, nutrient-poor, and heavy metal-rich growth medium. Our study proposes an ecological approach using a rhizobacterial consortium with synergistic effects in PGP and phytoremediation. Furthermore, is represents an important step towards understanding plant-rhizobacterial interactions in the rhizosphere.

REFERENCES

1. Upadhyay SK, Srivastava AK, Rajput VD, Chauhan PK, Bhojiya AA, Jain D, Chaubey G, Dwivedi P, Sharma B, Minkina T. Root exudates: Mechanistic insight of plant growth promoting rhizobacteria for sustainable crop production. Front Microbiol. 2022;13:916488.
   https://doi.org/10.3389/fmicb.2022.916488
2. Vocciante M, Grifoni M, Fusini D, Petruzzelli G, Franchi E. The role of plant growth-promoting rhizobacteria (PGPR) in mitigating plant's environmental stresses. Appl Sci. 2022;12(3):1231. https://doi.org/10.3390/app12031231
3. Souza RD, Ambrosini A, Passaglia LM. Plant growth-promoting bacteria as inoculants in agricultural soils. Genet Mol Biol. 2015;38:401-19.
   https://doi.org/10.1590/S1415-475738420150053
4. Wang G, Zhang Q, Du W, Ai F, Yin Y, Ji R, Guo H. Microbial communities in the rhizosphere of different willow genotypes affect phytoremediation potential in Cd contaminated soil. Sci Total Environ. 2021;769:145224.
   https://doi.org/10.1016/j.scitotenv.2021.145224
5. Khanna K, Jamwal VL, Gandhi SG, Ohri P, Bhardwaj R. Metal resistant PGPR lowered Cd uptake and expression of metal transporter genes with improved growth and photosynthetic pigments in Lycopersicon esculentum under metal toxicity. Sci Rep. 2019;9(1):5855.
   https://doi.org/10.1038/s41598-019-41899-3

6. Awan SA, Ilyas N, Khan I, Raza MA, Rehman AU, Rizwan M, Rastogi A, Tariq R, Brestic M. *Bacillus siamensis* reduces cadmium accumulation and improves growth and antioxidant defense system in two wheat (*Triticum aestivum* L.) varieties. Plants. 2020;9(7):878.
https://doi.org/10.3390/plants9070878

7. Mitra S, Pramanik K, Sarkar A, Ghosh PK, Soren T, Maiti TK. Bioaccumulation of cadmium by *Enterobacter* sp. and enhancement of rice seedling growth under cadmium stress. Ecotoxicol Environ Saf. 2018;156:183-96.
https://doi.org/10.1016/j.ecoenv.2018.03.001

8. He X, Xu M, Wei Q, Tang M, Guan L, Lou L, Xu X, Hu Z, Chen Y, Shen Z, Xia X. Promotion of growth and phytoextraction of cadmium and lead in *Solanum nigrum* L. mediated by plant-growth-promoting rhizobacteria. Ecotoxicol Environ Saf. 2020;205:111333.
https://doi.org/10.1016/j.ecoenv.2020.111333

9. Ma Y, Rajkumar M, Oliveira RS, Zhang C, Freitas H. Potential of plant beneficial bacteria and arbuscular mycorrhizal fungi in phytoremediation of metal-contaminated saline soils. J Hazard Mater. 2019;379:120813.
https://doi.org/10.1016/j.jhazmat.2019.120813

10. Han H, Sheng X, Hu J, He L, Wang Q. Metal-immobilizing *Serratia liquefaciens* CL-1 and *Bacillus thuringiensis* X30 increase biomass and reduce heavy metal accumulation of radish under field conditions. Ecotoxicol Environ Saf. 2018;161:526-33. https://doi.org/10.1016/j.ecoenv.2018.06.033

11. Etesami H. Bacterial mediated alleviation of heavy metal stress and decreased accumulation of metals in plant tissues: mechanisms and future prospects. Ecotoxicol Environ Saf. 2018;147:175-91. https://doi.org/10.1016/j.ecoenv.2017.08.032

12. Wang Y, Narayanan M, Shi X, Chen X, Li Z, Natarajan D, Ma Y. Plant growth-promoting bacteria in metal-contaminated soil: Current perspectives on remediation mechanisms. Front Microbiol. 2022;13:966226.
https://doi.org/10.3389/fmicb.2022.966226

13. Andrejić G, Šinžar-Sekulić J, Prica M, Dželetović Ž, Rakić T. Phytoremediation potential and physiological response of *Miscanthus× giganteus* cultivated on fertilized and non-fertilized flotation tailings. Environ Sci Pollut Res. 2019;26:34658-69. https://doi.org/10.1007/s11356-019-06543-7

14. Nurzhanova A, Pidlisnyuk V, Abit K, Nurzhanov C, Kenessov B, Stefanovska T, Erickson L. Comparative assessment of using *Miscanthus× giganteus* for remediation of soils contaminated by heavy metals: a case of military and mining sites. Environ Sci Pollut Res. 2019;26:13320-33.
https://doi.org/10.1007/s11356-019-04707-z

15. Spence AK, Boddu J, Wang D, James B, Swaminathan K, Moose SP, Long SP. Transcriptional responses indicate maintenance of photosynthetic proteins as key to the exceptional chilling tolerance of C4 photosynthesis in *Miscanthus× giganteus*. J Exp Bot. 2014;65(13):3737-47. https://doi.org/10.1093/jxb/eru209

16. Nebeská D, Trögl J, Ševcǔ A, Špánek R, Marková K, Davis L, Burdová. *Miscanthus x giganteus* role in phytodegradation and changes in bacterial community of soil contaminated by petroleum industry. Ecotoxicol. Environ. Saf. 2021;224:112630.
https://doi.org/10.1016/j.ecoenv.2021.112630

17. Nedjimi B. Phytoremediation: a sustainable environmental technology for heavy metals decontamination. SN Appl Sci. 2021;3(3):286. https://doi.org/10.1007/s42452-021-04301-4

18. Fernando A, Oliveira JS. Effects on growth, productivity, and biomass quality of *Miscanthus x giganteus* of soils contaminated with heavy metals. In: Willibrordus P. M. van Swaaij, editor. Proceedings: 2nd World Conference on Biomass for Energy, Industry and Climate Protection; 2004 May 10-14; Rome, Italy. Florence: ETA; 2004. p. 387-90.

19. Alves ARA, Yin Q, Oliveira RS, Silva EF, Novo LAB. Plant growth-promoting bacteria in phytoremediation of metal-polluted soils: Current knowledge and future directions. Sci Total Environ. 2022;838:156435.
https://doi.org/10.1016/j.scitotenv.2022.156435

20. Ma Y, Rajkumar M, Zhang C, Freitas H. Inoculation of Brassica oxyrrhina with plant growth promoting bacteria for the improvement of heavy metal phytoremediation under drought conditions. J Hazard Mater. 2016; 320:36-44.
https://doi.org/10.1016/j.jhazmat.2016.08.009

21. Zadel U, Nesme J, Michalke B, Vestergaard G, Płaza GA, Schröder P, Radl V, Schloter M. Changes induced by heavy metals in the plant-associated microbiome of *Miscanthus x giganteus*. Sci Total Environ. 2020;711:134433.
https://doi.org/10.1016/j.scitotenv.2019.134433

22. Pidlisnyuk V, Mamirova A, Pranaw K, Shapoval PY, Trögl J, Nurzhanova A. Potential role of plant growth-promoting bacteria in *Miscanthus x giganteus* phytotechnology applied to the trace elements contaminated soils. Int Biodeterior Biodegrad. 2020;155:105103.
https://doi.org/10.1016/j.ibiod.2020.105103

23. Rakić T, Pešić M, Kostić N, Andrejić G, Fira D, Dželetović Ž, Stanković S, Lozo J. Rhizobacteria associated with *Miscanthus x giganteus* improve metal accumulation and plant growth in the flotation tailings. Plant Soil. 2021;462:349-63.
https://doi.org/10.1007/s11104-021-04865-5

24. Cock PJ, Fields CJ, Goto N, Heuer ML, Rice PM. The Sanger FASTQ file format for sequences with quality scores, and the Solexa/Illumina FASTQ variants. Nucleic Acids Res. 2010;38(6):1767-71. https://doi.org/10.1093/nar/gkp1137

25. Erlich Y, Mitra PP, Delabastide M, McCombie WR, Hannon GJ. Alta-Cyclic: a self-optimizing base caller for next-generation sequencing. Nat Methods. 2008;5(8):679-82.
https://doi.org/10.1038/nmeth.1230

26. Jiang L, Schlesinger F, Davis CA, Zhang Y, Li R, Salit M, Gingeras TR, Oliver B. Synthetic spike-in standards for RNA-seq experiments. Genome Res. 2011;21(9):1543-51.
http://doi.org/10.1101/gr.121095.111

27. Trapnell C, Williams BA, Pertea G, Mortazavi A, Kwan G, van Baren MJ, Salzberg SL, Wold BJ, Pachter L. Transcript assembly and quantification by RNA-Seq reveals unannotated transcripts and isoform switching during cell differentiation. Nat Biotechnol. 2010;28(5):511-5.
https://doi.org/10.1038/nbt.1621

28. Dillies MA, Rau A, Aubert J, Hennequet-Antier C, Jeanmougin M, Servant N, Keime C, Marot G, Castel D, Estelle J, Guernec G, Jagla B, Jouneau L, Laloë D, Gall CL, Schaëffer B, Crom SL, Guedj M, Jaffrézic F; Consortium FS. A comprehensive evaluation of normalization methods for Illumina high-throughput RNA sequencing data analysis. Briefings Bioinf. 2013;14(6):671-83. https://doi.org/10.1093/bib/bbs046

29. Anders S, Huber W. Differential expression analysis for sequence count data. Genome Biol. 2010;11:R106.
https://doi.org/10.1186/gb-2010-11-10-r106

30. Robinson MD, McCarthy DJ, Smyth GK. edgeR: a Bioconductor package for differential expression analysis of digital gene expression data. Bioinformatics, 2010;26(1):139-40. https://doi.org/10.1093/bioinformatics/btp616

31. Kanehisa M, Goto S. KEGG: kyoto encyclopedia of genes and genomes. Nucleic Acids Res. 2000;28(1):27-30. https://doi.org/10.1093/nar/28.1.27

32. Yu G, Wang LG, Han Y, He QY. clusterProfiler: an R package for comparing biological themes among gene clusters. OMICS. 2012;16(5):284-7. https://doi.org/10.1089/omi.2011.0118

33. Pfaffl MW. A new mathematical model for relative quantification in real-time RT–PCR. Nucleic Acids Res. 2000;29(9):e45. https://doi.org/10.1093/nar/29.9.e45

34. Miao J, Feng Q, Li Y, Zhao Q, Zhou C, Lu H, Fan D, Yan J, Lu Y, Tian Q, Li W, Weng Q, Zhang L, Zhao Y, Huang T, Li L, Huang X, Sang T, Han B. Chromosome-scale assembly and analysis of biomass crop *Miscanthus lutarioriparius* genome. Nature Commun. 2021;12(1):2458. https://doi.org/10.1038/s41467-021-22738-4

35. Zhang W, Liao L, Xu J, Han Y, Li L. Genome-wide identification, characterization and expression analysis of MATE family genes in apple (*Malus× domestica* Borkh). BMC Genomics, 2021;22(1):632. https://doi.org/10.1186/s12864-021-07943-1

36. Niu E, Shang X, Cheng C, Bao J, Zeng Y, Cai C, Du X, Guo W. Comprehensive analysis of the COBRA-Like (COBL) gene family in gossypium identifies two COBLs potentially associated with fiber quality. PloS one, 2015;10(12):e0145725. https://doi.org/10.1371/journal.pone.0145725

37. Hunter JD. Matplotlib: A 2D graphics environment. Comput Sci Eng. 2007;9(03):90-5. https://doi.org/10.1109/MCSE.2007.55

38. Virtanen P, Gommers R, Oliphant TE, Haberland M, Reddy T, Cournapeau D, Burovski E, Peterson P, Weckesser W, Bright J, van der Walt SJ, Brett M, Wilson J, Millman KJ, Mayorov N, Nelson ARJ, Jones E, Kern R, Larson E, Carey CJ, Polat İ, Feng Y, Moore EW, VanderPlas J, Laxalde D, Perktold J, Cimrman R, Henriksen I, Quintero EA, Harris CR, Archibald AM, Ribeiro AH, Pedregosa F, van Mulbregt P. SciPy 1.0: fundamental algorithms for scientific computing in Python. Nat Methods. 2020;17(3):261-72. https://doi.org/10.1038/s41592-019-0686-2

39. Lin H, Wang Z, Liu C, Dong Y. Technologies for removing heavy metal from contaminated soils on farmland: A review. Chemosphere, 2022;305:135457. https://doi.org/10.1016/j.chemosphere.2022.135457

40. Yan A, Wang Y, Tan SN, Mohd Yusof ML, Ghosh S, Chen Z. Phytoremediation: a promising approach for revegetation of heavy metal-polluted land. Front Plant Sci. 2020;11:359. https://doi.org/10.3389/fpls.2020.00359

41. Wu B, Luo S, Luo H, Huang H, Xu F, Feng S, Xu H. Improved phytoremediation of heavy metal contaminated soils by *Miscanthus floridulus* under a varied rhizosphere ecological characteristic. Sci Total Environ. 2022;808:151995. https://doi.org/10.1016/j.scitotenv.2021.151995

42. Navazas A, Mesa V, Thijs S, Fuente-Maqueda F, Vangronsveld J, Peláez AI, Cuypers A, González. Bacterial inoculant-assisted phytoremediation affects trace element uptake and metabolite content in *Salix atrocinerea*. Sci Total Environ. 2022;820:153088. https://doi.org/10.1016/j.scitotenv.2022.153088

43. Ezaki B, Nagao E, Yamamoto Y, Nakashima S, Enomoto T. Wild plants, *Andropogon virginicus* L. and *Miscanthus sinensis* Anders, are tolerant to multiple stresses including aluminum, heavy metals and oxidative stresses. Plant Cell Rep. 2008;27(5):951-61. https://doi.org/10.1007/s00299-007-0503-8

44. Al Souki KS, Liné C, Douay F, Pourrut B. Response of three *Miscanthus × giganteus* cultivars to toxic elements stress: part 1, plant defence mechanisms. Plants 2021;10(10):2035. https://doi.org/10.3390/plants10102035

45. Hu R, Yu C, Wang X, Jia C, Pei S, He K, He G, Kong Y, Zhou G. *De novo* transcriptome analysis of *Miscanthus lutarioriparius* identifies candidate genes in rhizome development. Front Plant Sci. 2017;8:492. https://doi.org/10.3389/fpls.2017.00492

46. Nie G, Zhong M, Cai J, Yang X, Zhou J, Appiah C, Tang M, Wang X, Feng G, Huang L, Zhang X. Transcriptome characterization of candidate genes related to chromium uptake, transport, and accumulation in *Miscanthus sinensis*. Ecotoxicol Environ Saf. 2021;221:112445. https://doi.org/10.1016/j.ecoenv.2021.112445

47. Santos ALD, Chaves-Silva S, Yang L, Maia LGS, Chalfun-Júnior A, Sinharoy S, Zhao J, Benedito VA. Global analysis of the *MATE* gene family of metabolite transporters in tomato. BMC Plant Biol. 2017;17:185. https://doi.org/10.1186/s12870-017-1115-2

48. Du Z, Su Q, Wu Z, Huang Z, Bao J, Li J, Tu H, Zeng C, Fu J, He H. Genome-wide characterization of MATE gene family and expression profiles in response to abiotic stresses in rice (*Oryza sativa*). BMC Ecol Evol. 2021;21(1):141. https://doi.org/10.1186/s12862-021-01873-y

49. Huang Y, He G, Tian W, Li D, Meng L, Wu D, He T. Genome-wide identification of MATE gene family in potato (*Solanum tuberosum* L.) and expression analysis in heavy metal stress. Front Gen. 2021;12:650500. https://doi.org/10.3389/fgene.2021.650500

50. Xu L, Shen ZL, Chen W, Si GY, Meng Y, Guo N, Sun X, Cai YP, Lin Y, Gao JS. Phylogenetic analysis of upland cotton MATE gene family reveals a conserved subfamily involved in transport of proanthocyanidins. Mol Biol Rep. 2019;46:161-175. https://doi.org/10.1007/s11033-018-4457-4

51. Tiwari M, Sharma D, Singh M, Tripathi RD, Trivedi PK. Expression of OsMATE1 and OsMATE2 alters development, stress responses and pathogen susceptibility in *Arabidopsis*. Sci Rep. 2014;4:3964. https://doi.org/10.1038/srep03964

52. Liu J, Li Y, Wang W, Gai J, Li Y. Genome-wide analysis of MATE transporters and expression patterns of a subgroup of *MATE* genes in response to aluminum toxicity in soybean. BMC Genomics. 2016;17:223. https://doi.org/10.1186/s12864-016-2559-8

53. Li L, He Z, Pandey GK, Tsuchiya T, Luan S. Functional cloning and characterization of a plant efflux carrier for multidrug and heavy metal detoxification. J Biol Chem. 2002;277(7):5360-8. https://doi.org/10.1074/jbc.M108777200

54. Guo H, Hong C, Xiao M, Chen X, Chen H, Zheng B, Jiang D. Real-time kinetics of cadmium transport and transcriptomic

analysis in low cadmium accumulator *Miscanthus sacchariflorus*. Planta. 2016;244(6):1289-302.
https://doi.org/10.1007/s00425-016-2578-3

55. Sivaguru M, Liu J, Kochian LV. Targeted expression of *SbMATE* in the root distal transition zone is responsible for *Sorghum* aluminum resistance. Plant J. 2013;76(2):297-307.
https://doi.org/10.1111/tpj.12290

56. Li P, Liu Y, Tan W, Chen J, Zhu M, Lv Y, Liu Y, Yu S, Zhang W, Cai H. Brittle culm 1 encodes a COBRA-like protein involved in secondary cell wall cellulose biosynthesis in *Sorghum*. Plant Cell Physiol. 2019;60(4):788-801.
https://doi.org/10.1093/pcp/pcy246

57. Ahmed MZ, Alqahtani AS, Nasr FA, Alsufyani SA. Comprehensive analysis of the *COBRA-like* (*COBL*) gene family through whole-genome analysis of land plants. Genet Resour Crop Evol. 2024;71:863-72.
https://doi.org/10.1007/s10722-023-01667-9

58. Zaheer M, Rehman SU, Khan SH, Shahid S, Rasheed A, Naz R, Sajjad M. Characterization of new *COBRA like* (*COBL*) genes in wheat (*Triticum aestivum*) and their expression analysis under drought stress. Mol Biol Rep. 2022;49(2):1379-87.
https://doi.org/10.1007/s11033-021-06971-0

59. Bahmani R, Kim D, Modareszadeh M, Hwang S. Cadmium enhances root hair elongation through reactive oxygen species in *Arabidopsis*. Environ Experim Botany. 2022;196:104813.
https://doi.org/10.1016/j.envexpbot.2022.104813

60. Barling A, Swaminathan K, Mitros T, James BT, Morris J, Ngamboma O, Hall MC, Kirkpatrick J, Alabagy M, Spence AK, Hudson ME, Rokhsar DS, Moose SP. A detailed gene expression study of the *Miscanthus* genus reveals changes in the transcriptome associated with the rejuvenation of spring rhizomes. BMC Genomics. 2013;14:864.
https://doi.org/10.1186/1471-2164-14-864

SUPPLEMENTARY MATERIAL

Supplementary Table S1. Primer sequences for qPCR validation of RNA sequencing results.

Gene	Forward primer	Reverse primer	Reference
MATE 14	5'-CGTCACAGCACATCTTGGGC-3'	5'-GCATCCTCGGGCAATACCTGAT-3'	This study
MATE 40	5'-GGTGATCGGGGGAACCATGA-3'	5'-CCTGGCTTTCTCCACCTCCTTG-3'	This study
COBRA-like protein 1	5'-CCAGGAAGCTGTGTAGAGGGT-3'	5'-ACTAGAGGCGCCAAGCTGTT-3'	This study
Chitinase-like protein 1	5'-GCGAGCAGCAGGAGATCGAG-3'	5'-GCCTTGGTGAGCACGTTCCT-3'	This study
Sb02g041180	5'-TGAGAAAGCTCGGCAGGAAGCATA-3'	5'-TCTTCACCACAGATGTACGCACCA-3'	[60]

Supplementary Table S2. Uptake indexes (mg) in plant organs of *M. x giganteus* from two experimental groups (mix and control) for different metals were calculated as mean metal concentration (mg/kg DW) x mean dry weight (kg).

| Heavy metal	Leaf		Stem		Rhizome		Root	
	control	mix	control	mix	control	mix	control	mix
Mn	0.026	0.423	0.100	0.506	0.896	0.902	0.310	0.293
Pb	0.001	0.031	0.008	0.050	n.d.*	n.d.*	0.124	0.104
Zn	0.004	0.052	0.017	0.118	0.777	1.115	0.115	0.095
Ni	0.001	0.010	0.002	0.011	n.d.	0.007	0.060	0.053
Cu	0.001	0.009	0.002	0.004	0.006	0.020	0.028	0.049
Cr	0.001	0.022	0.005	0.021	0.088	0.089	0.061	0.024
Cd	0.000	0.001	0.000	0.002	0.001	0.009	0.003	0.003

* n.d. – not detectable

Supplementary Table S3. Translocation factors (TLF) and bioconcentration factors (BCF) for different metals in *M. x giganteus* from two experimental groups (mix and control).

Heavy metal	TLFcontrol	TLFmix	BCFcontrol	BCFmix
Mn	0.41	3.17	0.003	0.003
Pb	0.07	0.79	<0.001	<0.001
Zn	0.18	1.79	<0.001	<0.001
Ni	0.04	0.38	0.015	0.013
Cu	0.12	0.26	<0.001	<0.001
Cr	0.11	1.81	<0.001	<0.001
Cd	0.07	1.39	0.001	0.001

Supplementary Table S4. Summary of RNA-sequencing.

Samples	Control	Mix
Raw reads	21146651	22713862
Clean reads	20826287	22469139
Q20 (%)	97.18	97.25
Q30(%)	92.52	92.72
GC content (%)	54.8	53.6
Total mapped (%)	87.36	87.07
Uniquely mapped (%)	78.53	77.20
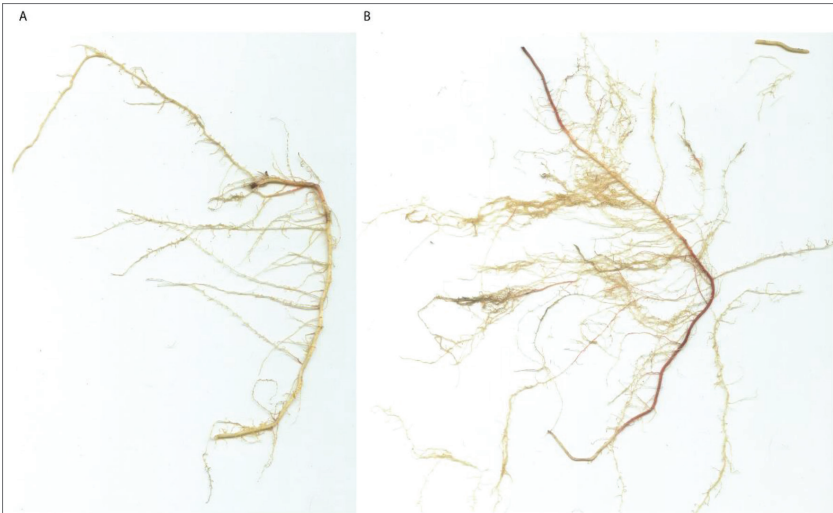
Supplementary Fig. S1. Roots of control (**A**) and mix (**B**) plants.

Supplementary Fig. S2. Evolutionary analysis of MATE proteins by Maximum Likelihood method. The evolutionary history was inferred by using the Maximum Likelihood method and JTT matrix-based model [1]. The tree with the highest log likelihood (-21783.62) is shown. Initial tree(s) for the heuristic search were obtained automatically by applying Neighbor-Join and BioNJ algorithms to a matrix of estimated pairwise distances using a JTT model and then selecting the topology with superior log likelihood value. The tree is drawn to scale, with branch lengths measured in the number of substitutions per site. This analysis involved 105 amino acid sequences. All positions containing gaps and missing data were eliminated (complete deletion option). There was a total of 188 positions in the final dataset. Evolutionary analyses were conducted in MEGA X [2].
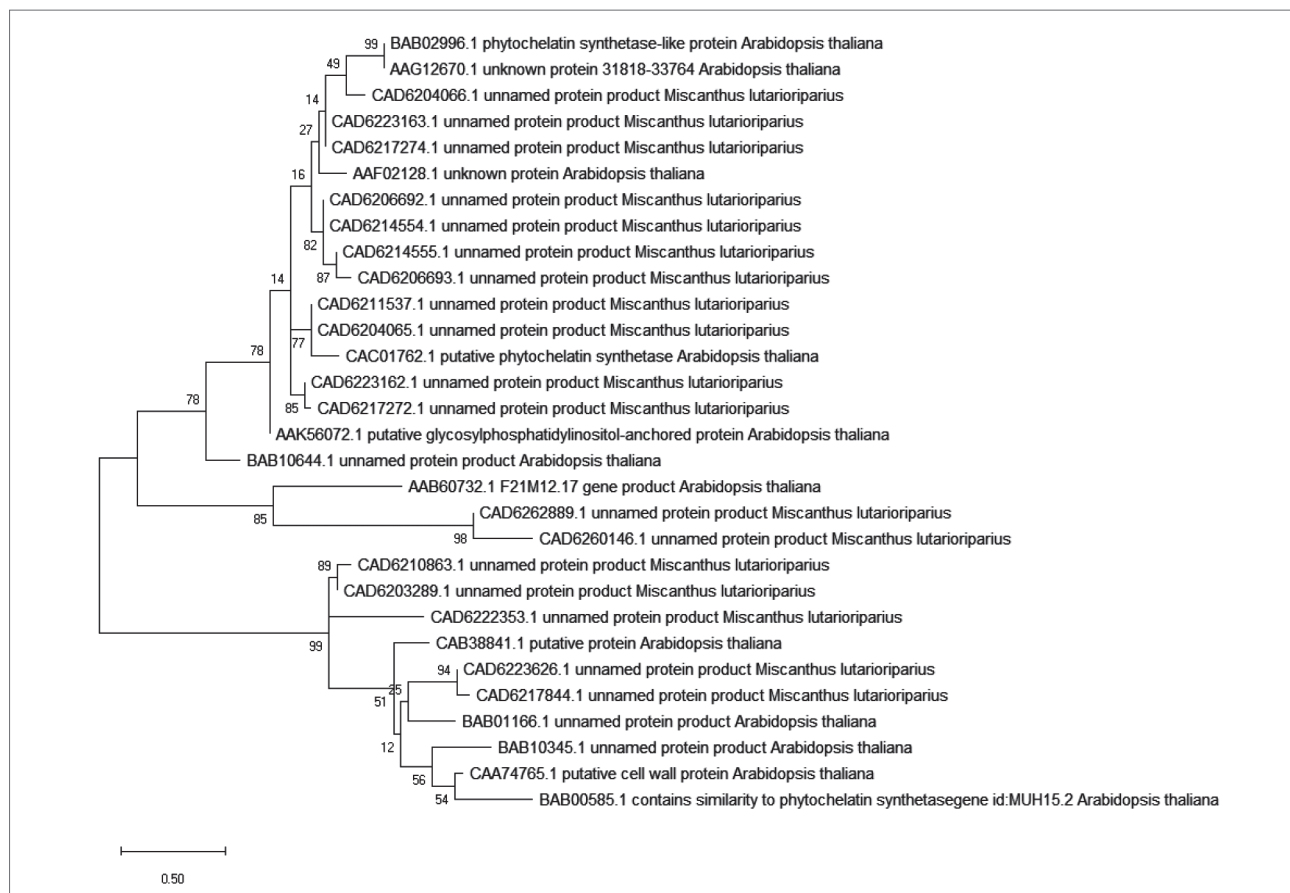
Supplementary Fig. S3. Evolutionary analysis of COBRA-like proteins by Maximum Likelihood method. The evolutionary history was inferred by using the Maximum Likelihood method and JTT matrix-based model [1]. The tree with the highest log likelihood (-956.04) is shown. The percentage of trees in which the associated taxa clustered together is shown next to the branches. Initial tree(s) for the heuristic search were obtained automatically by applying Neighbor-Join and BioNJ algorithms to a matrix of estimated pairwise distances using a JTT model and then selecting the topology with superior log likelihood value. The tree is drawn to scale, with branch lengths measured in the number of substitutions per site. This analysis involved 30 amino acid sequences. All positions containing gaps and missing data were eliminated (complete deletion option). There was a total of 32 positions in the final dataset. Evolutionary analyses were conducted in MEGA X [2].